

PALUSTRINE-LACUSTRINE AND ALLUVIAL FACIES OF THE (NORIAN) OWL ROCK FORMATION (CHINLE GROUP), FOUR CORNERS REGION, SOUTHWESTERN U.S.A: IMPLICATIONS FOR LATE TRIASSIC PALEOCLIMATE

LAWRENCE H. TANNER

*Department of Geography and Geosciences, Bloomsburg University, Bloomsburg, Pennsylvania 17815, U.S.A.
e-mail: lhtann@planetx.bloomu.edu*

ABSTRACT: The Upper Triassic (Norian) Owl Rock Formation was deposited in a low-gradient floodbasin at a subtropical paleolatitude. The lower part of the formation consists predominantly of fine-grained siliciclastic lithofacies deposited by sheetflood and sinuous streams on a muddy floodplain during a period of continuous basin aggradation. Nodular calcretes are increasingly mature higher in the formation, suggesting increasingly episodic depositional conditions. The upper part of the formation consists mostly of interbedded fine-grained siliciclastic facies and laterally continuous ledges of limestone and sandstone. The predominant limestone facies has brecciated to peloidal fabrics, spar-filled circumgranular cracks, and root channeling. The subordinate limestone facies displays wavy to irregular argillaceous lamination, desiccation cracks, and oscillation ripples, and is vertically and laterally gradational with the brecciated facies. The upper Owl Rock Formation records deposition of aggrading sequences of alluvial sediments deposited during base-level rise, capped by highstand carbonates deposited in small perennial and ephemeral carbonate lakes and ponds. Base-level lowstand in an overall semiarid climate resulted in extensive pedogenesis of the limestone and laterally equivalent alluvial facies. Basin wide variations in base level are interpreted as resulting from climatic fluctuations. This depositional model is consistent with an interpreted trend towards aridification on the Colorado Plateau during the Late Triassic as Pangea drifted northward from one climate zone to another.

INTRODUCTION

Interest in Upper Triassic lake deposits stems from the documented cyclicity of some of these deposits and the interpretation of orbital controls on cyclical deposition (Van Houten 1964; Olsen 1986; Gierlowski-Kordesch and Rust 1994; Olsen and Kent 1996; Clemmensen et al. 1998). Also of interest is the coincidence of deposition with the northward drift and breakup of Pangea, with consequent effects on climate and sedimentation (Dubiel et al. 1991; Parrish 1993; Olsen 1997; Clemmensen et al. 1998). Palustrine, i.e., pedogenically modified marginal-lacustrine facies, are also recognized for their importance in the interpretation of conditions of subsidence, climate, base level, and clastic sediment supply during deposition (Freytet and Plaziat 1982; Platt 1989; Alonso-Zarza et al. 1992; Platt 1992; Platt and Wright 1992; Armenteros et al. 1997). This paper describes interbedded palustrine-lacustrine limestones and alluvial siliciclastic facies in the Upper Triassic Owl Rock Formation and discusses these beds in the context of Late Triassic climatic change in the Colorado Plateau region.

Most previous interpretations of the sedimentology of the Owl Rock Formation have focused on the laterally continuous limestones that are characteristic of the upper part of the formation, interpreting them as the deposits of large-scale perennial lakes occupying a basin centered on the Four Corners area (Blakey and Gubitosa 1983; Dubiel 1987, 1993, 1994; Dubiel et al. 1991). The apparent lateral continuity of the beds, the limited presence of laminated fabrics (Dubiel 1987, 1989b, 1993, 1994), and the presence of crayfish burrows in associated siliciclastic facies (Hasiotis and Mitchell 1989; Hasiotis and Dubiel 1993), have suggested widespread deposition of carbonate in stable fresh-water lakes that periodically shrank. This interpretation supports a model of a humid, but seasonal, tropical

climate across the Colorado Plateau during Late Triassic time (Dubiel et al. 1991; Parrish 1993; Dubiel 1994). A contrasting interpretation suggests that the limestones are mature calcretes (up to Stage VI of Machette 1985), with little lacustrine influence, formed during a period of overall aridity (Lucas and Anderson 1993; Lucas et al. 1997). Support for this interpretation includes a paucity of typical lacustrine fauna, a lack of open lacustrine fabrics, the prominence of nodular and pisoidal fabrics in many of the limestone beds, and the presence of micritic nodules and root casts and traces in the intervening mudstones.

The importance of the paleoclimatic interpretation of the Owl Rock Formation derives from its stratigraphic position relative to other Chinle Group formations for which paleoclimate information is available. The Owl Rock Formation is underlain by alluvial strata of the Petrified Forest Formation, which display features suggesting deposition during subhumid conditions (Dubiel et al. 1991; Parrish 1993; Dubiel 1994). The Owl Rock Formation is, in turn, overlain unconformably by playa mudstone and eolian sandstone facies of the Rock Point Formation, succeeded by the predominantly eolian strata of the (Hettangian) Wingate Formation. Therefore, the interval of Owl Rock deposition represents either a period of increased humidity before the onset of aridity that was characteristic of the end of Triassic and beginning of Jurassic time or part of a transitional interval from more humid conditions prevalent at the onset of Chinle deposition to these more arid conditions. This uncertainty results largely from a lack of detailed descriptive sedimentology. This paper attempts to improve the understanding of Late Triassic climate through careful consideration of the Owl Rock lithofacies.

GEOLOGICAL SETTING

The designation Owl Rock Formation is used here following the revisions of Lucas (1993) and Lucas et al. (1997), who raised the former Chinle Formation to group status in part to unify the disparate lithostratigraphic nomenclature of the Four Corners region (Fig. 1). Deposition of Chinle Group strata, now exposed across much of the Colorado Plateau (Fig. 2), occurred in a continental back-arc basin (the Chinle basin) that extended from southwestern Texas to northern Wyoming (Lucas et al. 1997). The Four Corners region (the convergence of the boundaries of Arizona, Colorado, New Mexico, and Utah) was located at less than 10° N during Late Triassic time (Scotese 1994; Molina-Garza et al. 1995; Kent and Olsen 1997). Streamflow to the northwest, mainly from the Mogollon Highlands (approximately 500 km to the south and southwest) and to a lesser degree from the Uncompahgre Highlands (200 to 300 km to the east and northeast), deposited sediment across a broad alluvial plain (Marzolf 1994). Lowering of base level during Late Carnian time caused incision into the underlying Moenkopi Group, forming the Tr-3 unconformity. Deposition of the Shinarump, Cameron, and Petrified Forest formations, and lateral equivalents, occurred during Late Carnian and Early to Middle Norian time (Lucas et al. 1997). The Owl Rock Formation rests conformably on the Painted Desert Member of the Petrified Forest Formation. The Rhaetian-age Rock Point Formation, which unconformably overlies the Owl Rock Formation, is in turn separated from the mainly Hettangian-age Wingate Formation by the J-0 unconformity. The alluvial architectural elements and stratigraphy of most of these formations have been studied in considerable

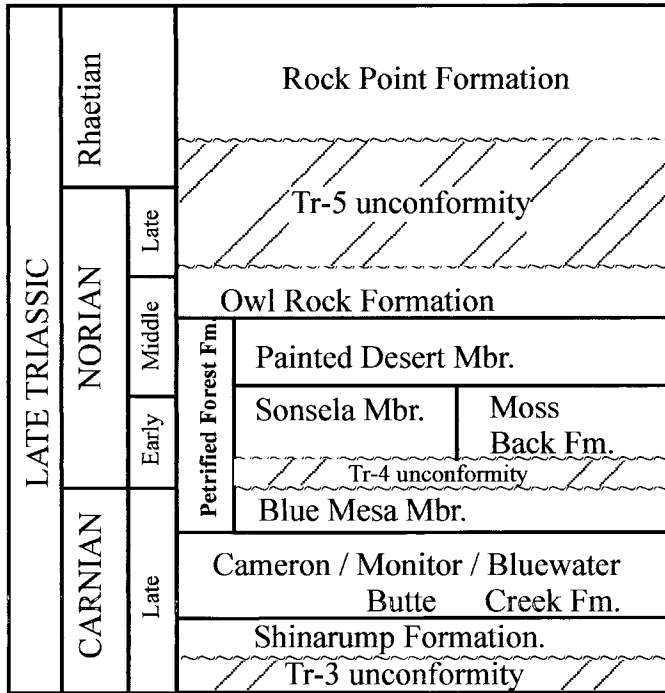


FIG. 1.—Stratigraphy of the Chinle Group in the Four Corners region, as defined by Lucas et al. (1997). Note: the designation Church Rock Member, previously considered equivalent to the former Rock Point Member, is now abandoned in favor of the present usage of Rock Point Formation.

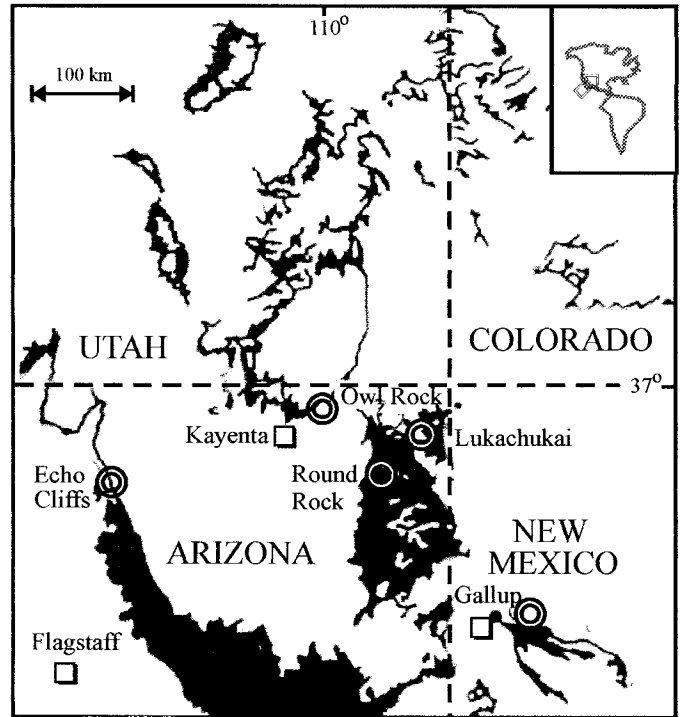


FIG. 2.—Location map illustrating areas of outcrop of Chinle Group strata (shaded) and locations of outcrops and roadcuts (circles) used in this study. Map adapted from Lucas (1993).

detail (Stewart et al. 1972; Bown et al. 1983; Kraus et al. 1984; Kraus and Middleton 1987; Dubiel 1987; Lucas 1993; Lucas et al. 1997).

The Owl Rock Formation comprises 70 to 150 m of interbedded siliciclastic and carbonate strata of approximately middle to late Norian age that crop out in northern Arizona, northwestern New Mexico, and southern Utah (Stewart et al. 1972; Lucas and Huber 1994). The formation is not recognized in southwestern Colorado, where the Rock Point Formation rests directly on the Petrified Forest Formation. The type locality for the formation is Owl Rock, located 10 km north of Kayenta, Arizona (Fig. 2). Although the general aspects of the Owl Rock Formation lithofacies have been described frequently in the literature (Dubiel 1987, 1989a, 1989b, 1993; Dubiel et al. 1991; Kirby 1993; Lucas et al. 1997), these descriptions provide few details of the sedimentology of the formation.

OWL ROCK LITHOFACIES

For this study, the Owl Rock Formation was examined at outcrop sections in cliffs and roadcuts in the Four Corners region at the Echo Cliffs, Owl Rock, Round Rock, and Lukachukai in northeastern Arizona, and Gallup, New Mexico (Fig. 2). The most complete section, measured at the type locality of Owl Rock, is presented here as representative of the vertical distribution of facies for this formation in the Four Corners region (Fig. 3). In the study area, the Owl Rock Formation grades upward from dominantly fine-grained siliciclastic facies at the base of the section to interbedded fine-grained siliciclastics and ledge-forming limestones and coarse siliciclastic facies higher in the section (Fig. 4). The uppermost part of the formation is dominated by limestone ledges up to 3 m thick. The ledges are laterally continuous for distances up to 2 km, but the aspect and thickness of individual beds within the ledges is variable over a scale of meters.

Siliciclastic Facies

Mudstone.—Thick illitic mudstone containing thin (< 1 m) interbedded siltstones and very fine-grained sandstones dominates the lower part of the

formation (0 to 50 m in the type section), forming well-weathered slopes. It is generally reddish-brown to orange, typically 10R5/4, and lacks organic matter. Much of the mudstone appears massive, but locally this facies displays ripple lamination, desiccation cracks, fine, drab-colored root traces, and meniscate-filled burrows. A variety of fabrics are observed in mudstone higher in the section, where interbedding with ledge-forming facies provides better exposure. Here, blocky fabrics, comprising blocky centimeter-scale peds with clay coatings, and brecciated fabrics (*sensu* Smoot and Olsen 1988) are present.

Micritic Nodule Horizons.—Mudstone-hosted calcareous nodule horizons are 0.3 to 1.8 m thick. Micritic nodules vary in shape from subspherical to irregularly globular (botryoidal), 2 to 7 cm in diameter, to vertically oriented, tuberoso, downward tapering forms up to 20 cm long. Nodules are commonly gray-green mottled (5GY8/1), contrasting with the host mudstone, and have an undifferentiated internal structure of micrite and millimeter-wide veins of sparry calcite (crystallaria). Nodular horizons in the lower 40 m of the type section comprise concentrations of isolated (noncoalescing) nodules. Horizons of coalescing nodules higher in the section commonly exhibit vertical stacking of nodules and prismatic fabric grading vertically to platy-laminar fabric (Fig. 5).

Burrowed Mudstone-Sandstone.—Dark-brown mudstone locally contains densely packed globular to elongate cylindrical casts, up to 1.5 m long, of calcareous sandy mudstone (Fig. 6). The cylinders have twisting and rare branching forms with smooth to knobby outer surfaces, tapering downward in some instances, and with a globular termination in others. The cylinders and nodules are often closely packed, forming irregular, nodular-weathering sandy mudstone to muddy sandstone lenses that are tens to hundreds of meters in outcrop length, have irregular bases, and are laterally gradational with the sandstone facies described below.

Sandstone and Conglomerate.—Very fine- to medium-grained sandstone occurs in ledge-forming beds, 0.2 to 3 m thick, that typically fine upwards. Sandstone beds in the lowermost 40 m of the type section are

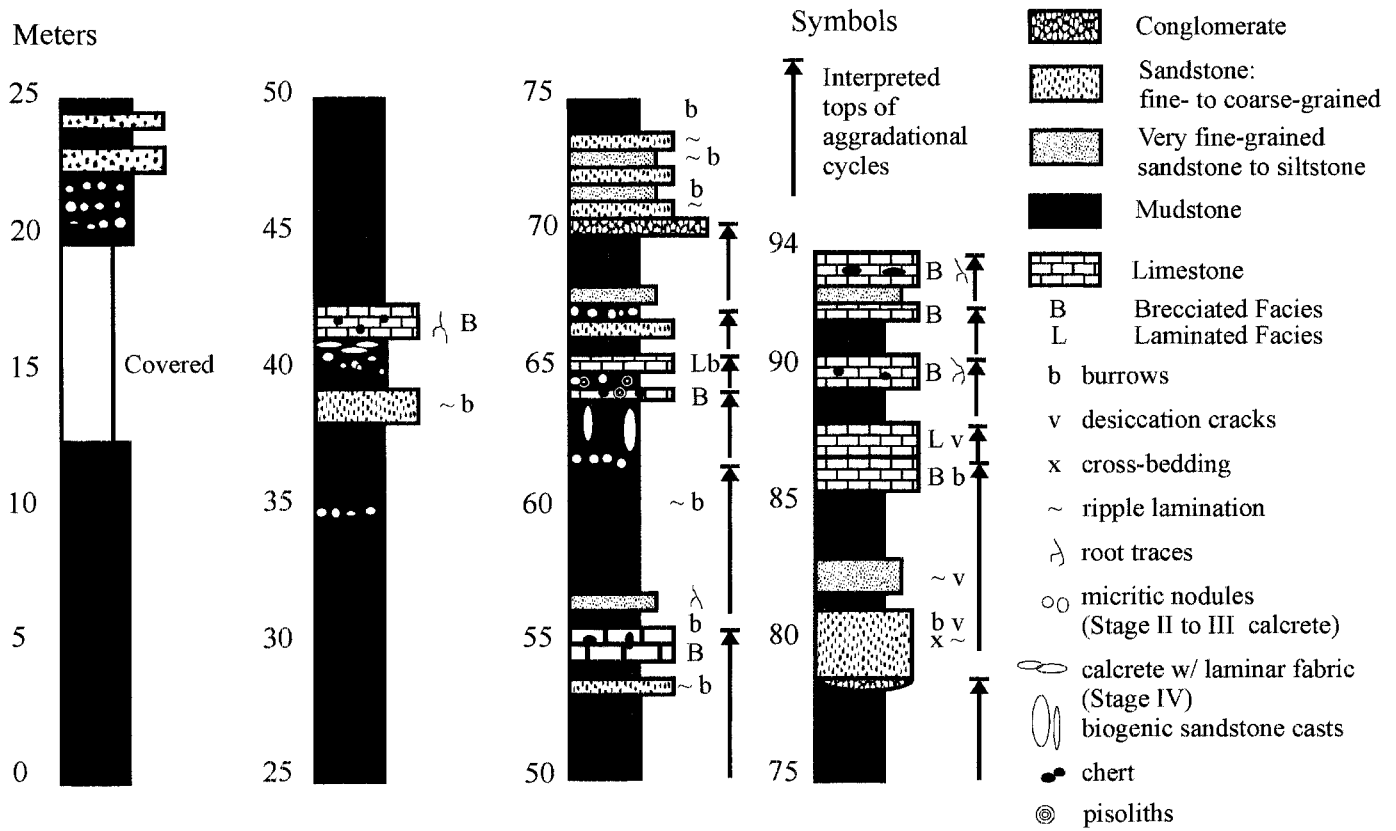


FIG. 3.—Stratigraphic section of the Owl Rock Formation measured at Owl Rock (Fig. 2). Base of the section was taken to be the top of a fluvial conglomerate bed overlying orange mudstone, assumed to represent the top of the underlying Painted Desert Member. Tops of interpreted aggradational cycles are seen at 42, 54, 62, 64, 65.5, 67, 85.5, 89, 92.5, and 94 m. In addition, conglomerate beds at 70 m and 79 m contain abundant reworked micritic nodules, presumably formed by downcutting through now-eroded sequence boundaries. Additional sequence tops may be concealed by poor exposure of the section below 50 m.

very fine grained and less than 1 m thick. The sandstone is composed predominantly of quartz with abundant mudstone aggregates (up to 12%) and is pervasively cemented by calcite. Many beds display trough cross-lamination to horizontal lamination and have ripple-laminated tops. Lateral accretion surfaces with 0.6 m of relief occur in one bed at the type section.

Internal scour-and-fill structures have relief of tens of centimeters. The lower contacts of most beds exhibit scouring into the underlying facies with relief up to 0.3 m. Bed thickness changes abruptly, and individual beds are continuous for distances of hundreds of meters. Many beds contain basal lag deposits of mudstone rip-up clasts, terrigenous pebbles, or pet-



FIG. 4.—View of the upper 70 m of the type section at Owl Rock. Top of the cliff corresponds to the top of the measured section (94 m). Labeled limestone ledges (L) correspond to limestone units at approximately 87, 65, 55, and 42 m in the measured section.



FIG. 5.—Stage IV calcrete profile (Machette 1985) displaying centimeter-scale, vertically stacked nodules with prismatic fabric, grading upward to platy fabric. Photograph from section in southern Echo Cliffs. Hammer for scale.



FIG. 6.—Lens of vertically elongate, downward-tapering sandstone casts hosted by mudstone, presumed formed by burrowing activity, possibly by crayfish (at 62 m in measured section). This lens overlies a calcrete nodule horizon. Scale is indicated by hammer.

rified wood. Vertical root traces up to 10 cm long penetrate the tops of some beds.

Conglomerate beds are 0.2 to 1.4 m thick and display matrix-supported to clast-supported fabrics comprising reddish-brown mudstone and gray-white micritic carbonate clasts, 0.5 to 6.0 cm in diameter. The beds have erosional bases and are laterally discontinuous, typically only tens of meters wide in outcrop, grading into sandstone. Color varies from reddish-brown to mottled purple. Structures in this facies include horizontal lamination, planar cross-bed sets up to 10 cm thick, and centimeter-scale scours filled by very fine-grained sandstone. Subhorizontal burrows, up to 10 cm long and 1 cm wide, are present in many beds.

Facies Interpretation.—The single-story nature, fining-upward fabric of many of the sandstone beds, and the presence of thin crossbed sets and lateral accretion surfaces suggest deposition of coarse (sand and gravel) siliciclastics by shallow (1 to 3 m deep), sinuous streams with downstream-migrating dunes and side-attached bars. The bedload of the streams contained mudstone and micritic intraclasts produced by lateral migration of the stream channel, and sand-size mud aggregates, possibly formed by pedogenic reworking of the muddy floodplain (Nanson et al. 1986; Rust and Nanson 1989, 1991; Gibling et al. 1998). Thin (0.2 to 0.3 m) wedge-shaped sandstones displaying ripple lamination, burrowing, and desiccation cracks may be levee deposits formed adjacent to the streams.

The limited presence of traction bedding in the mudstone facies suggests that some deposition may have taken place in shallow water, but the prevalence of pedogenic features, such as the blocky and brecciated fabrics, and the presence of calcrete (described below) indicates widespread sub-aerial exposure. Much of the mud may originally have been deposited by sheetflow on a broad, low-gradient floodplain crossed by shallow (< 1 m deep) channels. The abundance of mudstone aggregate grains in the coarser siliciclastic facies suggests that a substantial portion of the mud may have comprised pedogenically formed aggregates transported as bedload by traction currents.

Mudstone-hosted straight, vertical cylindrical casts in the Owl Rock Formation and other Chinle Group strata are interpreted as crayfish burrows (Dubiel et al. 1987; Hasiotis and Mitchell 1989), although the downward-tapering and branching form of some of these structures is also consistent with a root-cast origin. The lenses in which these structures occur are interpreted as the deposits of small, ephemeral ponds, possibly formed by channel avulsion, hosting fauna that were capable of burrowing down to the water table during seasonal periods of desiccation.

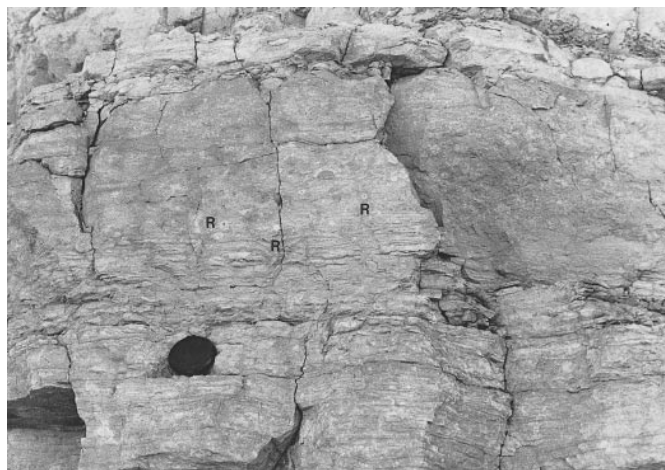


FIG. 7.—Laminated limestone facies with wavy to irregular partings at 82 m in measured section. Bed grades upward to mottled brecciated limestone facies with abundant root traces (R). Lens cap (50 mm) for scale.

Mudstone-hosted calcareous nodule horizons represent simple Stage II to IV calcrete profiles (Gile et al. 1966; Machette 1985). A pedogenic origin for these structures and fabrics is interpreted from the close resemblance to modern calcretes (Goudie 1983). Stage II profiles comprise isolated nodules in discrete horizons with gradational bases and tops. The more mature Stage III and IV profiles consist of coalesced horizons in which the nodules are commonly vertically stacked and display a prismatic fabric. Stage IV profiles grade upward from packed nodules to a platy-laminar fabric (Fig. 5). These profiles indicate exposure and nondeposition on the sediment surface for periods of 10^3 to 10^4 years (Machette 1985; Allen 1986). Stages III and IV profiles are typically erosionally truncated and overlain by coarse siliciclastic or limestone facies, and locally are laterally gradational with the brecciated limestone facies described below. Stage II profiles occur lower in the formation than the more mature Stage III and IV profiles. The overall trend of increasing paleosol maturity higher in the formation suggests a decreasing sedimentation rate and increasingly prolonged episodes of nondeposition, probably coincident with increased aridity.

The floodplain of the Channel Country in the Lake Eyre basin of Australia may be an appropriate modern analog for the mud-dominated part of the Owl Rock Formation. Here, sheetflood deposition of mud dominates the alluvial plain, through which flow sinuous to straight-channeled streams (Nanson et al. 1986; Gibling et al. 1998). Pedoturbation of the muddy floodplain by repeated wetting-drying cycles produces abundant mud aggregates, which may be redeposited by sheetflow or fluvial reworking following channel avulsion. Many features of the modern Channel Country are recognized in ancient formations (Gierlowski-Kordesch and Rust 1994; Talbot et al. 1994; Gierlowski-Kordesch and Huber 1995).

Limestone Facies

Laminated Limestone.—This facies is well developed only locally, and most beds grade vertically and laterally into the brecciated limestone facies described below. The lower contact of the beds is abrupt and commonly has relief of up to 20 cm. Beds of this facies are 0.6 to 0.8 m thick, tan to mottled reddish-brown in color, and are characterized by wavy to irregular laminae 0.2 to 0.5 cm thick (Fig. 7). Partings along these laminae expose bed surfaces that commonly display oscillation ripples, mud drapes, structureless horizontal burrows up to 3 cm long, and desiccation cracks penetrating downward up to 1 cm or more. Petrographically, this facies is characterized by dense micrite with wavy to ripple-form, argillaceous laminae, and spar-filled millimeter-scale fenestrae that are typically aligned parallel with the laminae (Fig. 8A). The laminae vary laterally and verti-

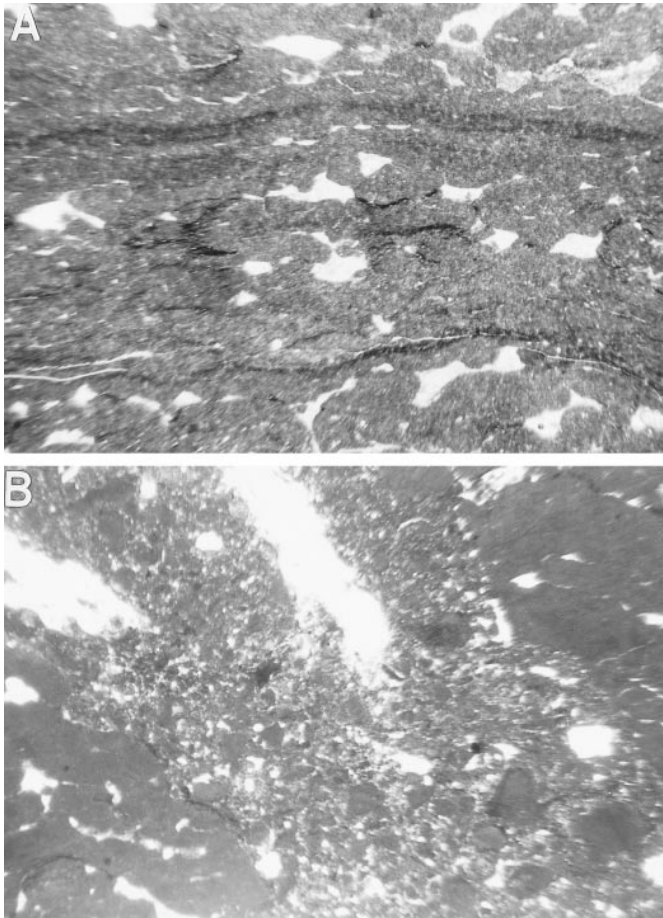


FIG. 8.—Aspects of the laminated limestone facies in thin section. Field of view in both photographs is 6 mm wide. **A)** Wavy argillaceous partings separate laminae comprising dense micrite with a partially peloidal fabric. Fenestrae and circumgranular cracks are filled by spar. **B)** Downward-tapering root trace in laminated limestone facies filled by siliclastic silt and micritic peloids.

cally in the degree of disruption by peloidal fabrics with sub-millimeter, spar-filled, circumgranular cracks. The upper parts of some beds of this facies are penetrated by downward-tapering root channels filled by a combination of micritic peloids and coarse spar (Figs. 7, 8B). Rare calcite pseudomorphs of gypsum laths occur in this facies.

Brecciated Limestone.—This is the predominant limestone facies and is well developed in the upper half of the formation throughout the study area. The ledges are continuous in outcrop for hundreds of meters, grading laterally to both calccrete and laminated limestone facies. The laminated facies also commonly grades vertically into the brecciated facies. Ledges of the brecciated facies comprise single-story or multi-story units, 0.4 to 1.6 m thick, of two to three beds. A variety of fabrics are common to most beds of this facies but are not present in every bed. A brecciated fabric throughout all or part of the bed is the most consistent characteristic of this facies (Fig. 9). This fabric comprises angular clast domains up to 10 cm in diameter, separated by millimeter-wide to centimeter-wide polygonal fractures. The clasts typically display an undifferentiated massive to rarely clotted-peloidal fabric comprising silty to slightly argillaceous micrite (Fig. 10). Spar-filled fenestrae occur locally within the clast domains. Some clasts exhibit weak pisolitic layering and ferrugination within the micrite. Where the fabric is peloidal, the peloids are separated by millimeter-scale circumgranular cracks filled by sparry calcite or chert and spherulitic chalcedony. Fractures between clasts are curved to straight, have vertical to horizontal orientations, and are filled variously by nonluminescent sparry



FIG. 9.—Typical bed of the brecciated limestone facies, at 94 m in the measured section. Dark mottling results from extensive replacement by chert. Downward-tapering root trace to the right of the hammer is filled mainly by spar.

calcite, calcite-cemented to chert-cemented siltstone, minor dolomite, or silty peloids that are either micritic or replaced by chert and spherulitic chalcedony.

Root traces commonly extend from the upper contact of beds and taper downward and bifurcate. These are subvertical and comprise millimeter-scale drab-gray filaments to fissures up to 20 cm long and 2 cm wide. They are filled variously by fine to coarse calcite spar, locally argillaceous, as well as peloids, silt, chert, and spherulitic chalcedony. Subhorizontal, non-tapering cylindrical burrows are 0.5 to 1.0 cm wide and up to 5 cm long. Chert locally replaces the infillings of burrows and root casts, and occurs in pisoliths and digitate masses up to 20 cm in diameter. Chert-filled vertical and horizontal fractures locally form a rectilinear pattern.

Most beds have a mottled appearance, varying from red-green to grayish purple-green to tan-gray, and contain isolated, weakly developed wavy lamination. Commonly, this lamination appears in the lower halves of beds of this facies and is gradational downward to weakly developed laminated facies (Fig. 11). In multi-story units, the tops of beds commonly display intense root penetration and brecciation that contrasts with lamination at the base of the overlying bed. The lower contact of this facies is abrupt and often irregular, with relief of 10 to 30 cm common over lateral dis-

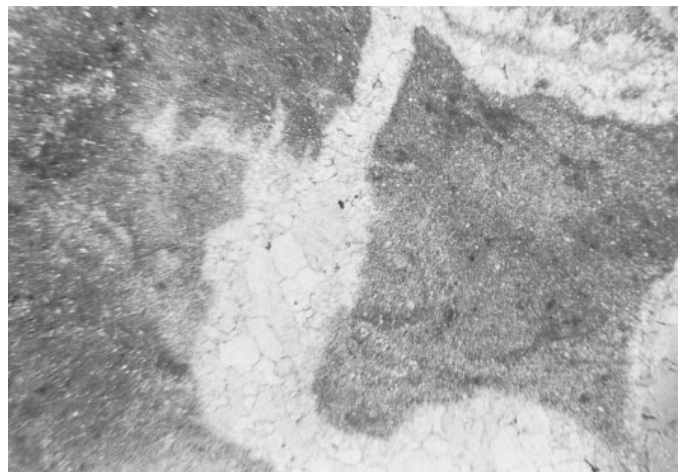


FIG. 10.—Typical appearance of the brecciated facies in thin section (field of view is 6 mm wide, polarizers crossed). Clast domains consist of silty, argillaceous micrite. Polygonal fractures are filled by coarse spar.



FIG. 11.—Bed of brecciated facies at 64 m in measured section. Relict lamination is visible in the middle of the bed. Centimeter-scale pisoliths (P) are visible in the lower one-third of the bed, some of which exhibit chert replacement (dark) to the left of the fissure. The size and abundance of fenestrae increase upward in the bed.

tances of several meters. Multi-story units comprise individual beds separated by irregular mudstone layers that are centimeters or less thick and commonly pinch out laterally, causing lateral amalgamation of the limestone beds.

Interpretation.—Body fossils and charophyte debris are largely absent in the laminated facies. Despite this lack, a lacustrine origin is suggested by the presence of fine argillaceous lamination and oscillation ripples. The presence of wave ripples and desiccation cracks combined with the distinct lack of high-energy shoreline (grainstone) or open lacustrine (wackestone) facies suggest that deposition took place in low-gradient lake systems with shallow depths, subject to episodic desiccation (Platt and Wright 1991; Alonzo-Zarza et al. 1992; Armenteros et al. 1997). The limited extent of the laminated facies and gradational nature of the contacts with the brecciated facies suggest that the lakes were small. Therefore, deposition of the carbonate is interpreted to have taken place in shallow carbonate lakes or ponds formed locally on the low-gradient floodplain. The nearly complete lack of evaporites indicates that the water in these lakes and ponds was only rarely saline. The argillaceous laminae may represent episodic incursions of siliciclastic sediment into the lake during floods. The clotted peloidal fabric and circumgranular cracking reflect minor pedogenic modification of the original carbonate textures during lake regression (Platt 1989, 1992). Subsequent phreatic cementation filled the circumgranular cracks with sparry cement. Examples of ancient carbonates displaying similar features that have been interpreted as alluvial-plain carbonate pond deposits include the Upper Triassic Mercia Mudstone Group of England (Talbot et al. 1994) and the Miocene Intermediate Unit of the Madrid Basin (Sanz et al. 1995).

The common association of the brecciated facies with the laminated facies clearly indicates formation of the former by modification of the latter. Microbrecciated–peloidal fabrics with circumgranular cracks, silt-filled fissures, and mottling, all common features of palustrine sediments (Platt 1989, 1992; Platt and Wright 1992; Armenteros et al. 1997), are common in the brecciated limestone facies of the Owl Rock Formation, suggesting a palustrine origin. The size and angularity of the clast domains in the brecciated facies indicate that they form by desiccation cracking and root penetration of the original sediments, a process capable of destroying delicate charophyte structures. The common circumgranular cracks and pisoliths result from shrinkage cracking and rotation during periods of emergence, typically under semiarid conditions (Platt and Wright 1992; Armenteros et al. 1997). Mottling resulted from vertical translocation of Fe oxides

and hydroxides during conditions of fluctuating water table or Eh and pH (Platt 1989). Local replacement of calcite by silica in meteoric waters formed chert. Many beds exhibit nearly vertical, downward-tapering channels or fissures with geopetal fills of silt and peloids, created by root penetration and solution enlargement, indicating extensive subaerial exposure. Irregular upper bed boundaries, locally with up to 20 cm of relief, but typically less than 10 cm, may have formed by incipient karstification. The common presence of lamination in the lower parts of beds of the brecciated facies suggests that the lamination is a relict depositional feature, and that the brecciated facies formed by modification of the tops of beds of the laminated facies.

The laminated and brecciated limestone facies are interbedded and gradational with the alluvial facies described above and represent deposition mainly in shallow perennial and ephemeral lakes and ponds occupying topographic lows on a broad floodplain. The laminated facies was deposited at the centers of these shallow lakes but was subject to episodic exposure during lake regression. The laterally equivalent, and commonly overlying, brecciated facies represents the broad, low-gradient margins of lakes that were subject to thorough pedogenic reworking during periods of lowstand when desiccation shrinkage and root penetration caused brecciation. The common vertical superposition of the brecciated and laminated facies further indicates complete desiccation of the lakes and consequent subaerial exposure and pedogenic reworking of the lake-bed sediments. Generally, the pervasiveness of the brecciation and the abundance of circumgranular cracking in this facies suggest pedogenesis under semiarid conditions (Platt and Wright 1992).

Stable-Isotope Analyses

Pedogenic nodules and lacustrine–palustrine carbonate facies were sampled for isotopic analysis by drilling lapped slabs with an ultrafine engraving tool while viewing under a binocular microscope. The samples were analyzed for ^{13}C and ^{18}O by Coastal Science Laboratories, Houston, Texas. Results are reported in ppt relative to PDB (Fig. 12A and appended). Massive micrite from five samples of pedogenic nodules from Echo Cliffs and Owl Rock contains carbonate with mean $\delta^{13}\text{C} = -7.4\text{‰}$ ($\sigma = 0.5$), and mean $\delta^{18}\text{O} = -5.7\text{‰}$ ($\sigma = 1.2$). Micrite from two samples of the laminated limestone facies at Owl Rock contains carbonate with mean $\delta^{13}\text{C} = -2.8\text{‰}$ ($\sigma = 0.0$), and mean $\delta^{18}\text{O} = -0.6\text{‰}$ ($\sigma = 0.1$). 16 samples of the brecciated facies from the Owl Rock section, mostly from the micritic clasts, contain carbonate with mean $\delta^{13}\text{C} = -4.5\text{‰}$ ($\sigma = 0.5$), and mean $\delta^{18}\text{O} = -2.7\text{‰}$ ($\sigma = 1.9$).

The limited overlap of the fields of standard deviation for these sample populations indicates carbonate precipitation under distinctly different conditions and/or from separate carbonate sources (Fig. 12B). Samples of pedogenic micrite appear to represent carbonate precipitated in a soil profile at equilibrium conditions with atmospheric CO_2 (Mora et al. 1993). The values reported here are consistent with other reported values from Late Triassic pedogenic calcretes (Suchecki et al. 1988; Cerling 1991; Tanner 1996). The composition of the laminated limestone facies represents the signature of lacustrine carbonate precipitated from evolved evaporation-enriched lacustrine waters (Talbot 1990; Platt 1992), consistent with the presence of (rare) calcite pseudomorphs of gypsum. The composition of the brecciated facies is generally intermediate between that of unaltered lacustrine and of pedogenic carbonate, suggesting mixing of isotopically heavy lacustrine carbonate with lighter carbonate precipitated in equilibrium with atmospheric CO_2 and/or meteoric groundwaters. The wide range of isotopic values for the brecciated facies reflects variations in carbonate available during multiple stages of carbonate precipitation, including the original (heavy) lacustrine carbonate, lighter pedogenic carbonate, and additional possible contributions from meteoric phreatic waters at a range of temperatures. Similar results have been described in other studies of the isotopic composition of palustrine carbonate (Platt 1989, 1992). One outlier

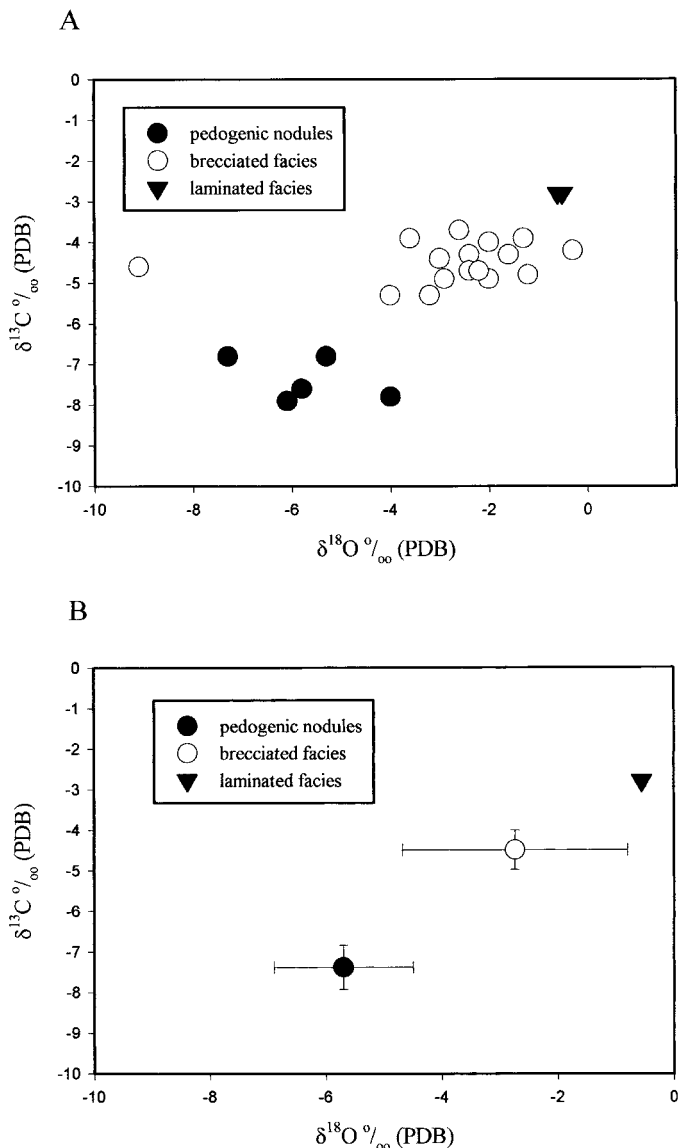


FIG. 12.—Isotopic analyses of carbonate from calcrete nodules and the brecciated and laminated facies of the Owl Rock Formation. **A)** Plotted raw data. **B)** Means for each sample group plotted with bidirectional standard deviation bars.

sample of the brecciated facies displays significantly depleted $\delta^{18}\text{O}$, possibly resulting from ^{18}O exchange with warmer formation waters. Mora et al. (1993) conclude that equilibration of oxygen, but not carbon, occurs in pedogenic carbonates during diagenesis.

FACIES SEQUENCE MODEL

Facies associations in the Owl Rock Formation indicate that deposition occurred in a broad, low-gradient floodbasin in which conditions changed with time. The lower 50 m of the formation consists mainly of fine-grained siliciclastic facies, contrasting with the alternating limestone and coarse- and fine-grained siliciclastic facies that comprise the uppermost 45 m. This difference suggests that a significant change occurred in the rate of sediment accumulation during deposition of this formation. The overall style of sedimentation in the Chinle Group may, in fact, reflect eustatically controlled variations in accommodation space. Deposition of the Petrified Forest Formation, for example, took place during a lowstand of sea level dur-

ing Late Carnian to Early Norian time (Haq et al. 1987) and is typified by deeply incised channels (Kraus and Middleton 1987). The low depositional gradient that is evident in the Owl Rock Formation is consistent with interpretations of a rising, eustatically controlled base level through Middle Norian time (Haq et al. 1987; Lucas and Huber 1994). The decline in the rate of aggradation evident in the upper part of the formation resulted from a decrease in accommodation space, consistent with declining sea level beginning in the Late Norian (Haq et al. 1987).

The vertical sequence of facies in the upper 45 m of the type section is interpreted as a series of aggradational sequences, punctuated by episodes of degradation. The sequences typically comprise fluvial channel sandstone and conglomerate bodies with erosional bases and associated floodplain mudstones, deposited during active sediment accumulation. The sequences are capped by lacustrine–palustrine limestones and laterally equivalent paleosols that formed as the siliciclastic sediment supply waned. The lacustrine–palustrine and laterally equivalent floodplain deposits were subjected to extended pedogenesis during prolonged episodes of nondeposition. In places, lacustrine–palustrine limestones abruptly overlie truncated calcareous paleosol horizons, suggesting an intervening erosional episode that resulted in a compressed sequence. In the type section (Fig. 3), 12 sequences are visible in the upper 45 m of the section (for which exposure is optimal), varying in thickness from 1.5 to 8.5 m.

These sequences may have resulted from a combination of autocyclic processes and base-level fluctuations with allocyclic controls. Similar sequences of interbedded siliciclastics and carbonates in ancient alluvial settings have been interpreted as the result of alluvial autocyclicality (Calvo et al. 1989; Sanz et al. 1995) in which carbonate deposition is attributed to episodic reduction of siliciclastic input into subenvironments that are isolated from the principal locus of deposition, such as interdistributary lows on a floodplain (Sanz et al. 1995). The commonly irregular nature of the lower contact of the carbonate beds in the Owl Rock Formation suggests that the water bodies in which carbonate accumulated formed in depressions created by fluvial processes. Lacustrine carbonate sedimentation was promoted in these water bodies by the lack of siliciclastic sediment input in areas distal from the main channels in an overall semiarid climate (Sanz et al. 1995). Channel avulsion and consequent migration of areas of floodplain aggradation is therefore likely to have controlled the location of contemporaneous deposition of siliciclastic and carbonate sediments.

Although alluvial systems have varied responses to base-level changes, aggradation during base-level rise is common as streams try to maintain constant gradient (Schumm 1993). But potential allocyclic controls on base level are varied, including eustasy, tectonics, and climatic control of basin hydrology, and not always discernible from the ancient record. Eustatic control of the aggradational sequences in the Owl Rock Formation is problematic. Although glacio-eustasy has been identified as a control on base level in Quaternary alluvial systems (Blum and Price 1988), the connection between eustasy and alluvial base level at great distance from shoreline is not clearly established (Ethridge et al. 1988; Schumm 1993; Rogers 1994). With 300 to 400 km separating the study area from the shoreline of the back-arc seaway (Marzolf 1994), high-frequency (fourth- or fifth-order) eustasy is unlikely to have controlled deposition of the Owl Rock aggradational sequences.

Variations in rates of uplift and subsidence have been cited as controls on base-level variations and channel avulsion during deposition of the Petrified Forest Formation (Kraus and Middleton 1987). Volcanic ash layers provide evidence of arc-magmatic activity, with consequent effects on source-area uplift, during deposition of the Petrified Forest Formation (Stewart et al. 1986), but there is no evidence for such activity in the Owl Rock Formation. Additionally, the fining-upward nature of the aggradational cycles and the lack of extrabasinal clasts in the conglomerate lithofacies of the Owl Rock Formation suggest that tectonic variations in source-area uplift or basin subsidence were not base-level controls (Schumm 1993; Rogers 1994).

Similar sequences of alternating alluvial mudstone and lacustrine-palustrine carbonates have been attributed to climatically driven base-level fluctuations (Talbot et al. 1994), with siliciclastic deposition dominating during lowstands and carbonate deposition occurring during highstands. The Owl Rock depositional sequences appear to have operated basinwide, and so may have resulted principally from fluctuating base level, driven by climate-controlled basin hydrology, modified locally by alluvial cyclicality. During periods of increased precipitation, fluvial discharge and sediment transport to the floodbasin increased, resulting in positive sediment accumulation and basinwide aggradation. These humid intervals also affected basin hydrology as ponding of water on the floodplain increased during peak base level, decreasing the fluvial gradient and sediment transport. Carbonates capped the aggradational sequences as small perennial and ephemeral lakes and ponds filled low areas on the floodplain created by stream migration and avulsion.

Extended periods of nondeposition and degradation occurred on the floodplain during base-level fall and lowstand as pedogenesis modified highstand deposits. Lacustrine and palustrine carbonate beds typically are intensely brecciated at the top, and are in turn overlain by mudstone or carbonate deposited during the succeeding base-level rise. Rising base level at the start of each succeeding sequence was accompanied by increased fluvial discharge, causing fluvial reworking and modest incision of the floodplain. The bedload of many of the streams consisted mainly of carbonate and mudstone intraclasts formed by floodplain erosion. The pedogenically modified limestones and laterally equivalent calcretes therefore represent the boundaries of base-level sequences. Calcretes interbedded in Upper Carboniferous cyclothem of the Sydney basin (Canada) have been interpreted similarly as lowstand surfaces (Tandon and Gibling 1997). Climatic fluctuations therefore may have controlled deposition of the aggradational cycles, while alluvial autocyclicality controlled the architecture and geometry of facies within the sequences, accounting for variations in sequence thickness.

Climate fluctuations across the Colorado Plateau region during Late Triassic time may have been controlled by strengthening and weakening of the monsoonal circulation system believed to have been operating across northern Pangea at this time (Kutzbach and Gallimore 1989; Dubiel et al. 1991). Orbital control of climate has been invoked for transgressive-regressive lacustrine cycles of the coeval Newark Supergroup (Olsen 1986; Olsen and Kent 1996). Computer modeling of Pangean climates has suggested that the precession cycle may have caused fluctuations in precipitation by as much as 25% above and below the mean in low-latitude regions (Kutzbach 1994), but the strict stratigraphic control necessary to test this hypothesis in the Owl Rock Formation is lacking.

LATE TRIASSIC CLIMATE CHANGE

The base-level changes resulting from climatic fluctuation became more pronounced with time as the regional climate shifted from subhumid to semiarid during Norian time. Drying of the climate of the Colorado Plateau region during the Late Triassic has been suggested previously from lithofacies and pedofacies transitions in Chinle Group strata (Dubiel 1994; Dubiel and Hasiotis 1994a, 1994b; Therrien et al. 1999). A humid but seasonal climate during the Late Carnian is indicated by gleyed kaolinitic and illuviated paleosols in strata of the Shinarump and Cameron formations (Dubiel and Hasiotis 1994a). The overlying Late Carnian to Middle Norian Petrified Forest Formation exhibits gleyed oxisols with weak vertic features in the Blue Mesa Member, succeeded by well-developed vertisols with pseudoanticlines and Stages I to III calcretes (Gile et al. 1966) in the Painted Desert Member (Herrick et al. 1999; Therrien et al. 1999). These features are indicative of a strongly seasonal but possibly subhumid climate (Therrien et al. 1999), consistent with paleogeographic reconstructions placing this area at subtropical latitudes during Late Triassic time (Kent and Olsen 1997). The Rock Point Formation, which unconformably over-

lies the Owl Rock Formation in the study area, consists of sandstones with interpreted fluvial and eolian sheet origins, and red mudstones with puffy-ground structures and sandpatch fabrics, interpreted as playa mudflat deposits (Welker et al. 1999). These strata were deposited during Rhaetic time, prior to deposition of the predominantly eolian (Hettangian) Wingate Formation (Dubiel 1989a; Dubiel and Hasiotis 1994a, 1994b; Lucas et al. 1997), providing evidence of increased aridity at the end of the Triassic.

Dubiel (1994) interprets a tropical monsoonal climate that persisted until the end of the Triassic, when northward migration of Pangea caused the breakup of the monsoonal circulation system. The occurrence of crayfish burrows and laterally persistent limestone beds in the Owl Rock Formation are interpreted as indicators of Late Triassic humidity; Parrish (1993) models a wet Late Triassic with reversed equatorial flow in an azonal monsoonal system based in part on this interpretation. However, crayfish burrowing is known in modern semiarid environments (Gibling et al. 1998), and the palustrine textures described in this paper are also indicative of semiaridity. Recognition of these palustrine limestones as the product of pedogenesis in a semiarid climate suggests gradual aridification on the Colorado Plateau through the entire Late Triassic. Strong seasonality, possibly recording a monsoonal influence, is consistent with depositional features in Upper Triassic strata of the Chinle Group, but this seasonality was not exclusive of climatic zonality. The progression from humid to semiarid climate recorded by Chinle Group strata is consistent with the drift of the Four Corners region from a subtropical humid zone toward a low-latitude belt of aridity. Owl Rock Formation carbonates therefore lend support to the model of a zonal, albeit highly seasonal, climate system for northern Pangea in the Late Triassic.

A coeval increase in aridity has been interpreted elsewhere from facies changes and paleosols in Upper Triassic to Lower Jurassic formations of the Newark Supergroup (Olsen 1997; Tanner in press). Olsen (1997) interprets climate change resulting from a 5° to 10° northward drift of Pangea between climate zones to explain an apparent trend of aridification in the basins of the Newark Supergroup. Additional support for a zonal climate model is found in the interpretation of a contemporaneous trend of increasing humidity in Upper Triassic strata of the Jameson basin as eastern Greenland drifted northward toward the humid mid-latitudes (Clemmensen et al. 1998).

CONCLUSIONS

Owl Rock Formation lithofacies were deposited in a low-gradient floodbasin during a period of increasing aridity. The lower part of the formation comprises fine-grained siliciclastic facies deposited on a muddy alluvial plain during conditions of relatively continuous basin aggradation. Calcrete profiles are increasingly mature stratigraphically upward, providing evidence for increasingly episodic sedimentation, probably resulting from climatic fluctuations that became larger with time. The upper Owl Rock Formation comprises sequences of fine and coarse alluvial siliciclastics deposited during episodes of aggradation, coinciding with base-level rise. The sequences are capped by palustrine-lacustrine limestones deposited during highstand in shallow, ephemeral lakes and ponds occupying topographic lows on the floodplain. Falling base level resulted in extensive pedogenic reworking of the sequence tops. The facies geometry within sequences was controlled locally by alluvial autocyclicality, but sequence boundaries were controlled basinwide by climatic fluctuations. Lithofacies and pedogenic features of the Owl Rock Formation are consistent with the interpretation from other Chinle Group Formations of a gradual transition from humid but strongly seasonal climate during the Early to Middle Norian to more arid conditions by the end of Triassic time.

ACKNOWLEDGMENTS

The author is indebted to S. Lucas for stimulating an interest in this problem and for time spent in the field with the author, and to J. DeAngelo and B. Welker for

assistance in the field. This work also benefited from fruitful discussions with E. Gierlowski-Kordesich and A. Alonso-Zarza. Thoughtful reviews and editorial assistance by J. Calvo, J. Hubert, and R. Renaut improved the clarity and focus of this article. Funding for this project was provided by a Research and Disciplinary Grant and a grant from the Special Initiative Fund, both of Bloomsburg University.

REFERENCES

- ALLEN, R.L., 1986, Pedogenic calcretes in the Old Red Sandstone facies (late Silurian—early Carboniferous) of the Anglo-Welsh area, southern Britain, in Wright, V.P., ed., *Paleosols: Their Recognition and Interpretation*: Boston, Blackwell Scientific, p. 58–86.
- ALONSO-ZARZA, A.M., CALVO, J.P., AND GARCÍA DEL CURA, M.A., 1992, Palustrine sedimentation and associated features—graïnification and pseudomicrokarst—in the Middle Miocene (Intermediate Unit) of the Madrid Basin, Spain: *Sedimentary Geology*, v. 76, p. 43–61.
- ARMENTEROS, I., DALEY, B., AND GARCIA, E., 1997, Lacustrine and palustrine facies in the Bembridge Limestone (late Eocene, Hampshire Basin) of the Isle of Wight, southern England: *Palaeogeography, Palaeoclimatology, Palaeoecology*, v. 128, p. 111–132.
- BLAKEY, R.C., AND GUBTOSA, R., 1983, Late Triassic paleogeography and depositional history of the Chinle Formation, southern Utah and northern Arizona, in Reynolds, M.W., and Dolly, E.D., eds., *Mesozoic Paleogeography of the West-Central United States*: Denver, Rocky Mountain Section SEPM, p. 57–76.
- BLUM, M.D., AND PRICE, D.M., 1988, Quaternary alluvial plain construction in response to glacio-eustatic and climate controls, Texas Gulf Coastal Plain, in Schanley, K.J., and McCabe, P.J., eds., *Relative Role of Eustacy, Climate and Tectonism in Continental Rocks*: SEPM, Special Publication 59, p. 31–48.
- BOWN, T.M., KRAUS, M.J., AND MIDDLETON, L.T., 1983, Triassic fluvial systems, Chinle Formation, Petrified Forest National Park, Arizona (abstract): Abstracts of Symposium on Southwest Geology and Paleontology, Flagstaff, Museum of Northern Arizona, p. 2.
- CALVO, J.P., ALONSO-ZARZA, A.M., AND GARCÍA DEL CURA, M.A., 1989, Models of Miocene marginal lacustrine sedimentation in response to varied depositional regimes and source areas in the Madrid Basin (central Spain): *Palaeogeography, Palaeoclimatology, Palaeoecology*, v. 70, p. 199–214.
- CERLING, T.E., 1991, Carbon dioxide in the atmosphere: evidence from Cenozoic and Mesozoic paleosols: *American Journal of Science*, v. 291, p. 377–400.
- CLEMMENSEN, L.B., KENT, D.V., AND JENKINS, F.A., JR., 1998, A Late Triassic lake system in East Greenland: facies, depositional cycles and paleoclimate: *Palaeogeography, Palaeoclimatology, Palaeoecology*, v. 140, p. 135–159.
- DUBIEL, R.F., 1987, Sedimentology of the Upper Triassic Chinle Formation, southeastern Utah [unpublished PhD thesis]: Boulder, Colorado, University of Colorado, 146 p.
- DUBIEL, R.F., 1989a, Depositional and paleoclimatic setting of the Upper Triassic Chinle Formation, Colorado Plateau, in Lucas, S.G., and Hunt, A.P., eds., *Dawn of the Age of the Dinosaurs in the American Southwest*: Albuquerque, New Mexico, New Mexico Museum of Natural History, p. 171–187.
- DUBIEL, R.F., 1989b, Sedimentology and revised nomenclature for the upper part of the Upper Triassic Chinle Formation and the Lower Jurassic Wingate Sandstone, northwestern New Mexico and northeastern Arizona: Albuquerque, New Mexico, New Mexico Geological Society, Guidebook 40, p. 213–223.
- DUBIEL, R.F., 1993, Depositional setting of the Owl Rock Member of the Upper Triassic Chinle Formation, Petrified Forest National Park and vicinity, Arizona, in Lucas, S.G., and Morales, M., eds., *The Nonmarine Triassic*: Albuquerque, New Mexico, New Mexico Museum of Natural History & Science Bulletin 3, p. 117–121.
- DUBIEL, R.F., 1994, Triassic deposystems, paleogeography, and paleoclimate of the Western Interior, in Caputo, M.V., Peterson, J.A., and Franczyk, K.J., eds., *Mesozoic Systems of the Rocky Mountain Region, USA*: Denver, Colorado, Rocky Mountain Section SEPM, p. 133–168.
- DUBIEL, R.F., AND HASIOTIS, S.T., 1994a, Paleosols and rhizofacies as indicators of climate change and groundwater fluctuations: the Upper Triassic Chinle Formation (abstract): Geological Society of America, Programs with Abstracts, v. 26, no. 6, p. 11–12.
- DUBIEL, R.F., AND HASIOTIS, S.T., 1994b, Integration of sedimentology, paleosols, and trace fossils for paleohydrologic and paleoclimatic interpretations in a Triassic tropical alluvial system (abstract): Geological Society of America, Abstracts with Programs, v. 26, no. 7, p. A-502.
- DUBIEL, R.F., BLODGETT, R.H., AND BOWN, T.M., 1987, Lungfish burrows in the Upper Triassic Chinle Formation, southeastern Utah and adjacent areas: *Journal of Sedimentary Petrology*, v. 57, p. 512–521.
- DUBIEL, R.F., PARRISH, J.T., PARRISH, J.M., AND GOOD, S.C., 1991, The Pangaea megamonsoon—evidence from the Upper Triassic Chinle Formation, Colorado Plateau: *Palaios*, v. 6, p. 347–370.
- ETHRIDGE, F.G., WOOD, L.J., AND SCHUMM, S.A., 1988, Cyclic variables controlling fluvial sequence development: problems and perspectives, in Schanley, K.J., and McCabe, P.J., eds., *Relative Role of Eustacy, Climate and Tectonism in Continental Rocks*: SEPM, Special Publication 59, p. 18–29.
- FREYET, P., AND PLAZIAT, J.-C., 1982, Continental carbonate sedimentation and pedogenesis—Late Cretaceous and Early Tertiary of southern France: Stuttgart, Germany, E. Schweizerbart'sche Verlagsbuchhandlung (Nägele u. Obermiller), Contributions to Sedimentology 12, 213 p.
- GIBLING, M.R., NANSON, G.C., AND MAROULIS, J.C., 1998, Anastomosing river sedimentation in the Channel Country of central Australia: *Sedimentology*, v. 45, p. 595–619.
- GIERLOWSKI-KORDESCH, E.H., AND HUBER, P., 1995, Lake sequences of the central Hartford Basin, Newark Supergroup: Connecticut State Geology Natural History Survey, Guidebook 7, p. B1–B35.
- GIERLOWSKI-KORDESCH, E., AND RUST, B.R., 1994, The Jurassic East Berlin Formation, Hartford Basin, Newark Supergroup (Connecticut and Massachusetts): a saline lake–playa–alluvial plain system, in Renaut, R., and Last, W.M., eds., *Sedimentology and Geochemistry of Modern and Ancient Saline Lakes*: SEPM, Special Publication 50, p. 249–265.
- GILE, L.H., PETERSON, F.F., AND GROSSMAN, R.B., 1966, Morphological and genetic sequences of accumulation in desert soils: *Soil Science*, v. 100, p. 347–360.
- GOUDIE, A.S., 1983, Calcrete, in Goudie, A.S., and Pye, K., eds., *Chemical Sediments and Geomorphology*: New York, Academic Press, p. 93–131.
- HAQ, B.U., HARDENBOL, J., AND VAIL, P.R., 1987, Chronology of fluctuating sea levels since the Triassic: *Science*, v. 235, p. 1156–1166.
- HASIOTIS, S.T., AND DUBIEL, R.F., 1993, Continental trace fossils of the Upper Triassic Chinle Formation, Petrified Forest National Park: *Petrified Forest National Park Newsletter*, no. 2, p. 8.
- HASIOTIS, S.T., AND MITCHELL, C.E., 1989, Lungfish burrows in the Upper Triassic Chinle and Dolores formations, Colorado Plateau—Discussion: new evidence suggests origin by a burrowing decapod crustacean: *Journal of Sedimentary Petrology*, v. 59, p. 871–875.
- HERRICK, A.S., JONES, M.M., THERRIEN, F., HOKE, G., AND FASTOVSKY, D.E., 1999, Late Triassic depositional systems and paleoenvironmental changes in Petrified Forest National Park, Arizona (abstract): Geological Society of America, Abstracts with Programs, v. 21, no. 2, p. A-23.
- KENT, D.V., AND OLSEN, P.E., 1997, Magnetostratigraphy and paleopoles from the Late Triassic Dan River–Danville basin: interbasin correlation of continental sediments and a test of the tectonic coherence of the Newark rift basins in eastern North America: *Geological Society of America, Bulletin*, v. 109, p. 366–379.
- KIRBY, R.E., 1993, Relationships of Late Triassic basin evolution and faunal replacement in the southwestern United States: perspectives from the upper part of the Chinle Formation in northern Arizona, in Lucas, S.G., and Morales, M., eds., *The Nonmarine Triassic*: New Mexico Museum of Natural History & Science, Bulletin 3, p. 233–242.
- KRAUS, M.J., AND MIDDLETON, L.T., 1987, Dissected paleotopography and base-level changes in a Triassic fluvial sequence: *Geology*, v. 15, p. 18–20.
- KRAUS, M.J., MIDDLETON, L.T., AND BOWN, T.M., 1984, Recognition of episodic base level changes in the fluvial Chinle Formation, Arizona (abstract): Geological Society of America, Abstracts with Programs, v. 16, p. 565.
- KUTZBACH, J.E., 1994, Idealized Pangean climates: sensitivity to orbital change, in Klein, G.D., ed., *Pangea: Paleoclimate, Tectonics, and Sedimentation During Accretion, Zenith, and Breakup of a Supercontinent*: Geological Society of America, Special Paper 288, p. 41–55.
- KUTZBACH, J.E., AND GALLIMORE, R.G., 1989, Pangean climates: Megamonsoons of the megacontinent: *Journal of Geophysical Research*, v. 94, p. 3341–3357.
- LUCAS, S.G., 1993, The Chinle Group: revised stratigraphy and chronology of Upper Triassic nonmarine strata in the western United States: *Museum of Northern Arizona, Bulletin* 59, p. 27–50.
- LUCAS, S.G., AND ANDERSON, O.J., 1993, Calcretes of the Upper Triassic Owl Rock Formation, Colorado Plateau, in Lucas, S.G. and Morales, M., eds., *The Nonmarine Triassic*: New Mexico Museum of Natural History & Science, Bulletin 3, p. G32–G41.
- LUCAS, S.G., AND HUBER, P., 1994, Sequence stratigraphic correlation of Upper Triassic marine and nonmarine strata, western United States and Europe, in Embry, A.F., Beauchamp, B., and Glass, D.J., eds., *Pangea: Global Environments and Resources*: Canadian Association Petroleum Geologists, Memoir 17, p. 241–254.
- LUCAS, S.G., HECKERT, A.B., ESTER, J.W., AND ANDERSON, O.J., 1997, Stratigraphy of the Upper Triassic Chinle Group, Four Corners region, in Mesozoic Geology and Paleontology of the Four Corners Region: New Mexico Geological Society, Guidebook 48, p. 81–108.
- MACHETTE, M.N., 1985, Calcic soils of the southwestern United States, in Weide, D.L., ed., *Soils and Quaternary Geology of the Southwest United States*: Geological Society of America, Special Paper 203, p. 1–21.
- MARZOLF, J.E., 1994, Reconstruction of the early Mesozoic Cordilleran cratonic margin adjacent to the Colorado Plateau, in Caputo, M.V., Peterson, J.A., and Franczyk, K.J., eds., *Mesozoic Systems of the Rocky Mountain Region, USA*: Denver, Colorado, Rocky Mountain Section SEPM, p. 181–215.
- MOLINA-GARZA, R.S., GEISSMAN, J.W., AND VAN DER VOO, R., 1995, Paleomagnetism of the Dockum Group (Upper Triassic), northwest Texas: further evidence for the J-1 cusp in the North American apparent polar wander path and implications for the apparent polar wander and Colorado Plateau migration: *Tectonics*, v. 14, p. 979–993.
- MORA, C.I., FASTOVSKY, D.E., AND DRIESE, S.G., 1993, Geochemistry and stable isotopes of paleosols: University of Tennessee, Department of Geological Sciences, Studies in Geology no. 23, 65 p.
- NANSON, G.C., RUST, B.R., AND TAYLOR, G., 1986, Coexistent mud braids and anastomosing channels in an arid-zone river: Cooper Creek, central Australia: *Geology*, v. 14, p. 175–178.
- OLSEN, P.E., 1986, A 40-million-year lake record of early Mesozoic climate forcing: *Science*, v. 234, p. 842–848.
- OLSEN, P.E., 1997, Stratigraphic record of the early Mesozoic breakup of Pangea in the Laurasia–Gondwana rift system: *Annual Review of Earth and Planetary Sciences*, v. 25, p. 337–401.
- OLSEN, P.E., AND KENT, D.V., 1996, Milankovitch forcing in the tropics of Pangea during the Late Triassic: *Palaeogeography, Palaeoclimatology, Palaeoecology*, v. 122, p. 1–26.
- PARRISH, J.T., 1993, Climate of the supercontinent Pangea: *Journal of Geology*, v. 101, p. 215–253.
- PLATT, N.H., 1989, Lacustrine carbonates and pedogenesis: sedimentology and origin of palustrine deposits from the Early Cretaceous Rupelo Formation, W Cameros Basin, N Spain: *Sedimentology*, v. 36, p. 665–684.
- PLATT, N.H., 1992, Fresh-water carbonates from the lower Freshwater Molasse (Oligocene,

- western Switzerland): sedimentology and stable isotopes: *Sedimentary Geology*, v. 78, p. 81–99.
- PLATT, N.H., AND WRIGHT, V.P., 1991, Lacustrine carbonates: facies models, facies distributions and hydrocarbon aspects, in Anadón, P., Cabrera, L., and Kelts, K., eds., *Lacustrine Facies Analysis: International Association of Sedimentologists, Special Publication 13*, p. 57–74.
- PLATT, N.H., AND WRIGHT, V.P., 1992, Palustrine carbonates and the Florida Everglades: towards an exposure index for the fresh-water environment?: *Journal of Sedimentary Petrology*, v. 62, p. 1058–1071.
- ROGERS, R.R., 1994, Nature and origin of through-going discontinuities in nonmarine foreland basin strata, Upper Cretaceous, Montana: Implications for sequence analysis: *Geology*, v. 22, p. 1119–1122.
- RUST, R.G., AND NANSON, G.C., 1989, Bedload transport of mud as pedogenic aggregates in modern and ancient rivers: *Sedimentology*, v. 36, p. 291–306.
- RUST, R.G., AND NANSON, G.C., 1991, Reply: Bedload transport of mud as pedogenic aggregates in modern and ancient rivers: *Sedimentology*, v. 38, p. 158–160.
- SANZ, M.E., ALONSO-ZARZA, A.M., AND CALVO, J.P., 1995, Carbonate pond deposits related to semi-arid alluvial systems: examples from the Tertiary Madrid Basin, Spain: *Sedimentology*, v. 42, p. 437–452.
- SCOTSE, C.R., 1994, Late Triassic paleogeographic map, in Klein, G.D., ed., *Pangea: Paleoclimate, Tectonics, and Sedimentation During Accretion, Zenith, and Breakup of a Supercontinent: Geological Society of America, Special Paper 288*, p. 7.
- SCHUMM, S.A., 1993, River response to baselevel changes: implications for sequence stratigraphy: *Journal of Geology*, v. 101, p. 279–294.
- SMOOT, J.P., AND OLSEN, P.E., 1988, Massive mudstones in basin analysis and paleoclimatic interpretation of the Newark Supergroup, in Manspeizer, W., ed., *Triassic–Jurassic Rifting, Continental Breakup, and the Formation of the Atlantic Ocean and Passive Margins, Part A: Amsterdam, Elsevier*, p. 249–274.
- STEWART, J.H., POOLE, F.G., AND WILSON, R.F., 1972, Stratigraphy and origin of the Chinle Formation and related Upper Triassic strata in the Colorado Plateau region: U.S. Geological Survey, Professional Paper 690, 336 p.
- STEWART, J.H., ANDERSON, T.H., HAXEL, G.B., SILVER, L.T., AND WRIGHT, J.E., 1986, Late Triassic paleogeography of the southern Cordillera: The problem of a source for voluminous volcanic detritus in the Chinle Formation of the Colorado Plateau region: *Geology*, v. 14, p. 567–570.
- SUCHECKI, R.K., HUBERT, J.F., AND DE WET, C.B., 1988, Isotopic imprint of climate and hydrogeochemistry on terrestrial strata of the Triassic–Jurassic Hartford and Fundy rift basins: *Journal of Sedimentary Petrology*, v. 58, p. 801–811.
- TALBOT, M.R., 1990, A review of the paleohydrological interpretation of carbon and oxygen isotopic ratios in primary lacustrine carbonates: *Chemical Geology*, v. 80, p. 261–279.
- TALBOT, M.R., HOLM, K., AND WILLIAMS, M.A.J., 1994, Sedimentation in low-gradient desert margin systems: A comparison of the Late Triassic of northwest Somerset (England) and the late Quaternary of east-central Australia, in Rosen, M.R., ed., *Paleoclimate and Basin Evolution of Playa Systems: Geological Society of America, Special Paper 289*, p. 97–117.
- TANDON, S.K., AND GIBLING, M.R., 1997, Calcretes at sequence boundaries in Upper Carboniferous cyclothems of the Sydney basin, Atlantic Canada: *Sedimentary Geology*, v. 112, p. 43–67.
- TANNER, L.H., in press, Pedogenic record of paleoclimate and basin evolution in the Triassic–Jurassic Fundy rift basin, eastern Canada, in LeTourneau, P., ed., *Aspects of Triassic–Jurassic Rift Basin Geoscience: New York, Columbia University Press*.
- TANNER, L.H., 1996, Pedogenic record of Early Jurassic climate in the Fundy rift basin, eastern Canada, in Morales, M., ed., *The Continental Jurassic: Museum of Northern Arizona, Bulletin 60*, p. 565–574.
- TERRIEN, F., HERRICK, A.S., JONES, M.M., HOKE, G.D., AND FASTOVSKY, D.E., 1999, Paleoenvironmental changes in the Chinle Formation as seen in vertebrate localities of the Petrified Forest National Park, Arizona (abstract): *Geological Society of America, Abstracts with Programs*, v. 31, no. 2, A-72.
- VAN HOUTEN, F.B., 1964, Cyclic lacustrine sedimentation, Upper Triassic Lockatong Formation, central New Jersey and adjacent Pennsylvania: *Geological Survey of Kansas, Bulletin 169*, p. 497–531.
- WELKER, B.H., DEANGELO, J.F., AND TANNER, L.H., 1999, Paleoenvironmental and paleoclimatic interpretations of the Upper Triassic Owl Rock and Rock Point Formations, Chinle Group, Four Corners Region (abstract): *Geological Society of America, Abstracts with Programs*, v. 31, no. 2, p. A-78.

Received 6 October 1999; accepted 17 March 2000.

APPENDIX—Stable-Isotope Analyses For Owl Rock Formation Carbonates

Sample Type	Sample Location	$\delta^{13}\text{C}$ (‰ PDB)	$\delta^{18}\text{O}$ (‰ PDB)
Pedogenic nodule	Echo Cliffs	–7.6	–5.1
“ ”	“ ”	–6.8	–7.3
“ ”	“ ”	–7.4	–5.4
“ ”	“ ”	–7.3	–4.6
“ ”	Owl Rock	–7.8	–4.0
Laminated facies	“ ”	–2.8	–0.6
“ ”	“ ”	–2.8	–0.5
Brecciated facies	“ ”	–4.3	–1.6
“ ”	“ ”	–4.7	–2.2
“ ”	“ ”	–5.3	–3.2
“ ”	“ ”	–4.9	–2.9
“ ”	“ ”	–3.9	–3.6
“ ”	“ ”	–4.0	–2.0
“ ”	“ ”	–4.3	–2.4
“ ”	“ ”	–4.8	–1.2
“ ”	“ ”	–4.6	–9.1
“ ”	“ ”	–4.4	–3.0
“ ”	“ ”	–4.9	–2.0
“ ”	“ ”	–3.7	–2.6
“ ”	“ ”	–5.3	–4.0
“ ”	“ ”	–3.9	–1.3
“ ”	“ ”	–4.2	–0.3
“ ”	“ ”	–4.7	–2.4